

Developing Brain Atlas through Deep Learning

Asim Iqbal^{1,2}, Romesa Khan³, Theofanis Karayannis^{1,2}

¹Laboratory of Neural Circuit Assembly, Brain Research Institute (HiFo), UZH

²Neuroscience Center Zurich (ZNZ), UZH/ETH Zurich

³Department of Biology (D-BIOL), ETH Zurich

*Correspondence should be addressed to T.K. (karayannis@hifo.uzh.ch)

Abstract

To uncover the organizational principles governing the human brain, neuroscientists are in need of developing high-throughput methods that can explore the structure and function of distinct brain regions using animal models. The first step towards this goal is to accurately register the regions of interest in a mouse brain, against a standard reference atlas, with minimum human supervision. The second step is to scale this approach to different animal ages, so as to also allow insights into normal and pathological brain development and aging. We introduce here a fully automated convolutional neural network-based method (*SeBRe*) for registration through Segmenting Brain Regions of interest in mice at different ages. We demonstrate the validity of our method on different mouse brain post-natal (P) developmental time points, across a range of neuronal markers. Our method outperforms the existing brain registration methods, and provides the minimum mean squared error (MSE) score on a mouse brain dataset. We propose that our deep learning-based registration method can (i) accelerate brain-wide exploration of region-specific changes in brain development and (ii) replace the existing complex brain registration methodology, by simply segmenting brain regions of interest for high-throughput brain-wide analysis.

With the development and efficient implementation of various methods in neuroscience for tracking specific populations of brain cells *in situ*, such as the generation of genetically modified animals, or the more conventional immunocytochemistry and mRNA in-situ hybridization (ISH) on brain tissue, neuroscientists are able to visualize the expression of various neuronal subtypes in different brain regions across development [1]. These cellular expression patterns are captured by high-throughput imaging techniques, such as whole tissue light-sheet microscopy, or wide bright field and fluorescent microscopy using high resolution slide scanners. With an ever-increasing interest from neuroscience labs in mesoscopic brain-wide analysis, there has been an exponential growth in large-scale brain datasets. However, quantification of neural density of various cell types in these brain datasets remains a great challenge in the field of neuroscience, primarily due to the complexity of registering mouse brain sections against a standard reference atlas.

A number of efforts are underway worldwide to develop high-throughput image registration frameworks for analyzing such large-scale brain datasets [2, 3]. Nevertheless, most of these frameworks are semi-manual, such that the user is either expected to set a certain range of parameters like intensity threshold, background contrast, etc. for every brain section or even completely transform their brain datasets into the framework-readable format. Notwithstanding that, these methods result in limited performance in registration of brain sections against a reference atlas, hence lacking the generalizability for analyzing a variety of datasets.

The development of deep learning-based techniques is now providing state-of-the-art results in real-world object classification [4], localization [5] and segmentation [6] tasks. Nevertheless, their usage in the analysis of complex brain image datasets has been scarce [7]. Amongst the many challenges, this Artificial Intelligence (AI)-based approach would require the generation of a large enough dataset of brain-sections that is 1) labelled with brain regions in reference to a standard mouse atlas and 2) captures the variability of various regions in different sections across the brain.

We propose that the task of registering brain sections against a standard reference atlas can also be achieved by segmenting the regions in the brain by feature engineering, using a deep neural network. Therefore, we introduce an unprecedented approach to the classical problem of brain image registration, ‘*registration through segmentation*’. This approach deploys a fully automated deep neural network-based method to segment and annotate various regions of the mouse brain at different stages of development, by optimization of Mask R-CNN (regions with convolutional neural network) architecture [6].

We first generated a human-annotated mouse brain regions dataset of 600 brain sections, using the Allen Brain Institute Online Public Resource (OPR), to train (2/3) and test (1/3) the performance of the network. By comparing the performance of our method with human-annotated ground-truth data, we achieve a high average precision (AP) score in lateral and medial sagittal sections of the mouse brain. We further demonstrate the power of our method in comparison to the traditional brain registration approaches. *SeBRe* achieves higher accuracy in the mouse brain registration task and provides a clear benefit of eliminating any additional need for the mouse brain atlas as a reference. In fact, our method, *SeBRe*, automatically generates the brain reference atlas corresponding to any input brain section. This approach marks a paradigm shift in dealing with large scale brain datasets, since it is independent of 1) the time-intensive step of manually selecting, followed by 2) the computationally expensive step of registering, the putative reference atlas onto brain sections. Therefore, we propose that our method of segmenting brain regions could potentially replace the classical affine and non-affine transformation approaches of registering brain sections against a standard mouse

reference atlas. The block diagram summary of our method is presented in **figure 1a**.

Performance on brain sections. Demonstration of *SeBRe*'s output on various sections of P14 mouse brains is shown in **figure 1b**. The first column shows the human-annotated masks for eight regions of interest in randomly selected mouse brain sections, labelled with GABAergic neuronal markers, GAD1 and VGAT. The middle column shows the performance of *SeBRe* in segmenting the eight regions in these brain sections. The right-most column shows performance of the network on rotated versions of the same brain sections. The network seems to perform adequately well in segmenting brain regions in upright as well as rotated versions of the brain sections. Performance of the network is optimal in most brain regions, including isocortex, hippocampus, basal ganglia, telencephalic vesicle and the midbrain. For segmenting pre-thalamus, performance of the network is limited due to a large variation in the structure and size of this region, as we move from lateral to medial across sagittal brain sections.

The mean average precision (AP) score for brain sections in the test dataset is 0.843. Although brain sections are randomly distributed across the training and testing datasets, it is observed that the network seems to perform better on lateral brain sections as compared to medial brain sections. The increased complexity and compactness of the brain regions in medial as compared to lateral planes, presents a bigger challenge for the network to segment these regions optimally.

Performance on untrained images of different markers at various ages. After testing the performance of our network on P14 brain sections, we further tested our method on various mouse brain sections across different developmental time points (P4, P14, P28 and P56), for commonly used neuronal markers (CaMKIIa, Nissl, GAD1 and VGAT) [8]. CaMKIIa labels the population of excitatory neurons, GAD1 and VGAT labels GABAergic neurons, and Nissl labels all the cells in the brain and is often used to explore the morphology of brain tissue. **Supplementary figure 6** shows the results of segmentation on various mouse brain sections, across different ages and neuronal markers. **Supplementary figure 6 (a-b)** includes randomly selected brain sections from a P4 mouse brain of GAD1 and VGAT. The network seems to perform optimally in segmenting isocortex, thalamus and the telencephalic vesicle, whereas detection of the midbrain and hindbrain regions proves a challenge for the network. **Supplementary figure 6 (c-d)** shows the performance of the network on randomly selected brain sections from Nissl and CaMKIIa brains at P4. Although, the network has been trained on GAD1 and VGAT tissue sections of only a single age (P14), it performs equally well in segmenting brain regions, for various neuronal markers at different developmental ages. **Supplementary figure 6 (g-j)** demonstrates the segmentation of P28+ mouse brain regions in GAD1, VGAT, CaMKIIa and Nissl brains. Similar to the P14 testing dataset, in the medial brain sections of older mice, the network seems to occasionally omit a few regions, such as the midbrain and pre-thalamus, but the segmentation of isocortex and other regions remains unaffected.

Comparison of *SeBRe* with other brain registration techniques. To demonstrate the power of our '*registration through segmentation*' approach, the performance of *SeBRe* was compared with two other commonly used image registration methods: elastix, a toolbox for rigid and non-rigid registration of medical images [9], and the Neurodata Registration module (ndreg), which uses affine and non-affine transformations to align a mouse brain reference atlas image to brain section images [10]. For fair comparison, a mouse brain reference atlas image, comprising only of the eight regions of interest on which *SeBRe* is trained, was registered onto the corresponding mouse brain section, using ndreg and elastix. **Figure 2a** visually demonstrates the registration performance of *SeBRe*, elastix and ndreg on lateral and medial sagittal sections from GAD1

and VGAT brains. Mean squared error (MSE) score for the ‘registered’ mask returned by *SeBRe* was notably lower than MSE scores of both elastix and ndreg, as shown in **figures 2b and 2c**, indicating higher registration accuracy achieved by our method. It is interesting to observe that these commonly used registration techniques make similar mistakes e.g. increased MSE score in registering rotated samples, in contrast to our machine intelligence-based method, *SeBRe* (**supplementary figure 7**).

In conclusion, we introduce a deep neural network-based method, *SeBRe* to classify and segment different regions in mouse brain images. To test the performance of our method, we utilize the open-source Allen Brain ISH data for two neuronal markers and generate a human-annotated masked dataset of 600 brain sections from two-week-old mice. We test the performance of our method on 1/3 of the dataset and demonstrate the proper and accurate segmentation of eight unique brain regions in mouse brain sections, lateral as well as medial sagittal planes. Importantly, this network performs optimally on images that differ in scale (up- or down-scaled), as well as in relative sizes of the brain regions. This would be the case not only at different stages of development, but also in tissue sections in which the proper geometry of the brain has been compromised due to methodological issues (e.g. during brain tissue slicing). This is demonstrated by the fact that although *SeBRe* was trained only on a P14 image dataset, the network performs equally well on other ages including P4, P28 and P56, as well as on rotated samples. Moreover, our method achieves a higher registration accuracy, as compared to existing classical brain image registration approaches. We believe that *SeBRe* can be a valuable tool for many biological applications, such as segmenting brain regions in microscopy images for brain-wide analysis in animal models, or even human pathophysiological samples/post-mortem tissue.

Author contributions

A.I., R.K. and T.K. conceptualized the study and wrote the paper. A.I and R.K. developed the *SeBRe* method and performed the quantitative comparison with other registration methods.

Competing interests

The authors declare no financially competing interests.

References

- [1] Lein, E.S. et al. (2007) Genome-wide atlas of gene expression in the adult mouse brain, *Nature* 445: 168-176. doi: 10.1038/nature05453.
- [2] Fürth, Daniel, et al. "An interactive framework for whole-brain maps at cellular resolution." *Nature neuroscience* 21.1 (2018): 139.
- [3] Niedworok, Christian J., et al. "aMAP is a validated pipeline for registration and segmentation of high-resolution mouse brain data." *Nature communications* 7 (2016): 11879.
- [4] Jarrett, Kevin, Koray Kavukcuoglu, and Yann LeCun. "What is the best multi-stage architecture for object recognition?" 12th International Conference on Computer Vision, 2009. IEEE, 2009.
- [5] Ren, Shaoqing, et al. "Faster r-cnn: Towards real-time object detection with region proposal networks." *Advances in neural information processing systems*. 2015.
- [6] He, Kaiming, et al. "Mask r-cnn." *IEEE International Conference on Computer Vision (ICCV)*, 2017. IEEE, 2017.
- [7] Milletari, Fausto, et al. "Hough-CNN: deep learning for segmentation of deep brain regions in MRI and ultrasound." *Computer Vision and Image Understanding* 164 (2017): 92-102.
- [8] © 2015 Allen Institute for Brain Science. Allen Brain Atlas API (brain-map.org/api/index.html)
- [9] S. Klein, M. Staring, K. Murphy, M.A. Viergever, J.P.W. Pluim, "elastix: a toolbox for intensity based medical image registration," *IEEE Transactions on Medical Imaging*, vol. 29, no. 1, pp. 196 - 205, January 2010.

- [10] D.P. Shamonin, E.E. Bron, B.P.F. Lelieveldt, M. Smits, S. Klein and M. Staring, "Fast Parallel Image Registration on CPU and GPU for Diagnostic Classification of Alzheimer's Disease", *Frontiers in Neuroinformatics*, vol. 7, no. 50, pp. 1-15, January 2014.
- [11] Boxy SVG editor (<https://boxy-svg.com/>)

Methods

Generating the ground-truth dataset. We generate the ground-truth dataset by first fetching the open-source In-Situ Hybridized (ISH) mouse brain images for two different genetic markers (GAD1 and VGAT), from the Allen Brain OPR [8]. These two markers capture the population of GABAergic neurons in developing mouse brains. We choose P14 as the intermediate age of animal that captures enough variance in terms of brain region development between a young animal pup (P4) and an adult mouse (P28+). These brain sections are cut at 20 μ m-thick in sagittal planes and each is 200 microns apart from the next, covering one hemisphere of a whole brain from lateral to medial. **Supplementary figure 1** shows sagittal sections of a GAD1 brain at P14, which were used for generating the ground-truth data. The brain sections are overlaid by the Allen developing mouse brain reference atlas, with each region assigned a unique color code. This was done by manually registering the brain sections with scalar vector graphics (SVG) files to the reference atlas, using Boxy SVG editor [11]. The SVG files of developing mouse brain atlas were imported from Allen Brain OPR. GAD1 and VGAT brains at P14 consist of 36 (17 and 19 respectively) brain sections. Six sections were removed from these two brains, as these did not meet the required quality criteria due to broken/damaged tissue. To increase the variability of the sample images, for each brain section, we introduce a synthetic variance of a 2° rotation with a range of [-20, 20], resulting in 20 rotated versions of each brain section. We apply the same procedure for all 30 brain sections, the resulting dataset comprised of 600 brain sections. We apply a down-sampling ratio of 25% on each image in the dataset. Out of these 30 sections, we randomly choose 2/3 of the brain sections with their rotated versions (400 images) for training and the remaining 1/3 with their rotated versions (200 images) for testing.

Generating masks for brain regions. To demonstrate the performance of *SeBRe*, we choose 8 major regions in the developing mouse brain for training and testing, namely: isocortex, hippocampus, basal ganglia, thalamus, prethalamus, midbrain, telencephalic vesicle (olfactory bulb and partial forebrain) and hindbrain (cerebellum). Sample binary masks of five example regions, along with their corresponding brain sections, are shown in **supplementary figure 2**. These masks are generated from the human-annotated ground-truth dataset, where each brain region is masked with a unique color code, as shown in **supplementary figure 1**.

Network architecture. *SeBRe* is designed by optimization of Mask R-CNN, constructed using a convolutional backbone that comprises of the first five stages of the very deep ResNet101 [12] and Feature Pyramid Network (FPN) [13] architectures, for feature extraction from the entire input brain section image, I [384 \times 384]. The network architecture is shown in **supplementary figure 3**. The feature map is processed by a Region Proposal Network (RPN), which applies a convolutional neural network over the feature map in a sliding-window fashion. The RPN segregates and forwards the predicted n potential Regions of Interest (RoI) from each window to the Mask R-CNN 'heads' based on the FPN. The RoI feature maps undergo a critical feature pooling operation by a pyramidal RoIAlign layer, which preserves a pixel-wise correspondence to the original image. Each level of the pyramidal RoIAlign layer is assigned a RoI feature map from the different levels of the FPN backbone, depending on the feature map area, returning n pooled feature maps, P_n [7 \times 7]. Three arms of the FPN perform

the core operations of brain region segmentation. The ‘classifier’ and ‘regressor’ heads, inherited from Faster R-CNN [5], detect and identify distinct brain regions, and compute region-specific bounding boxes. The classifier output layer returns a discrete probability distribution $[n, 9]$, for 9 different object classes (8 brain regions + background). The regressor output layer gives the 4 (x-coordinate, y-coordinate, width, height) bounding-box regression offsets to be applied for each class, per ROI $[n, (4 \times 8)]$. **Supplementary figure 4** illustrates the step by step procedure of brain region localization and classification, performed by the FPN heads ‘classifier’ and ‘regressor’ heads.

A fully convolutional network (FCN) forms the more recent mask-prediction arm, returning a binary mask spanning each segmented brain region. The mask arm applies a mask of resolution $m \times m$ for each class, for each ROI $[n, (8 \times m^2)]$. Respectively, the output of the backbone architecture and the mask head, for a single brain section is shown in **supplementary figure 5**. The network is trained using a stochastic gradient descent algorithm that minimizes a multi-task loss corresponding to each labeled ROI:

$$L = L_{cls} + L_{reg} + L_{mask}$$

where L_{cls} and L_{reg} are the region classification loss and bounding box regression loss, respectively, as defined below.

$$L(p_i, q_i) = \frac{1}{n_{cls}} \sum_i L_{cls}(p_i, p_i^*) + \mu \frac{1}{n_{reg}} \sum_i L_{reg}(q_i, q_i^*)$$

p_i is the probability of the i^{th} proposed ROI, or *anchor*, enclosing an object (anchors with greater than 0.7 Intersection-over-Union (IoU) overlap with a ground-truth bounding box are considered positive; anchors with less than 0.3 IoU overlap are considered negative). p_i^* denotes if the anchor is positive ($p_i^* = 1$) or negative ($p_i^* = 0$). Vector q_i represents the 4 coordinates characterizing the predicted anchor bounding box, whereas vector q_i^* represents the coordinates for the ground-truth box corresponding to a positive anchor. L_{cls} for each anchor is calculated as log loss for two class labels (object vs. non-object). L_{reg} is a regression loss function robust to outliers, as defined in [14]. n_{cls} and n_{reg} are the normalization parameters for classification and regression losses, respectively, weighted by a parameter μ [5]. L_{mask} is computed as average cross-entropy loss for per-pixel binary classification, applied to each ROI [6].

Implementation of *SeBRe*. The implementation of *SeBRe* generally follows the original work [6], with limited hyper-parameter optimization for the brain section dataset. Training on the brain section dataset is initialized with pre-trained weights for the MS COCO [15] dataset. Each batch slice consists of a single brain section image per GPU; batch normalization layers are inactivated, to optimize training for the small effective batch size. Training is performed using an NVIDIA GeForce GTX 970 GPU. The training regime comprises of two stages. First, the network heads are trained for 6000 iterations, at a learning rate of 0.001 and learning momentum of 0.9. In the second stage, all layers are fine-tuned for 9000 iterations, at a reduced learning rate of 0.0001. During inference, diverging from the original model, the mask branch is applied to the highest scoring 8 detection boxes, proposed by the RPN. The maximum number of ground truth instances detected per image is also limited to 8 (to avoid erroneous duplicate instances of region-specific masks). Adopting a more stringent approach, the minimum probability threshold for instance detection is raised to 0.9, in order to improve the accuracy of instance segmentation.

Software availability.

The code and datasets generated during and/or analysed during the current study are available from the corresponding author on reasonable request. *SeBRe* will be available online on bitbucket (<https://bitbucket.org/theolab/>) for the neuroscience community.

References

- [12] He, Kaiming, et al. "Deep residual learning for image recognition." Proceedings of the IEEE conference on computer vision and pattern recognition. 2016.
- [13] Lin, Tsung-Yi, et al. "Feature pyramid networks for object detection." CVPR. Vol. 1. No. 2. 2017.
- [14] R. Girshick, "Fast R-CNN," in IEEE International Conference on Computer Vision (ICCV), 2015.
- [15] Lin, Tsung-Yi, et al. "Microsoft coco: Common objects in context." European conference on computer vision. Springer, Cham, 2014.

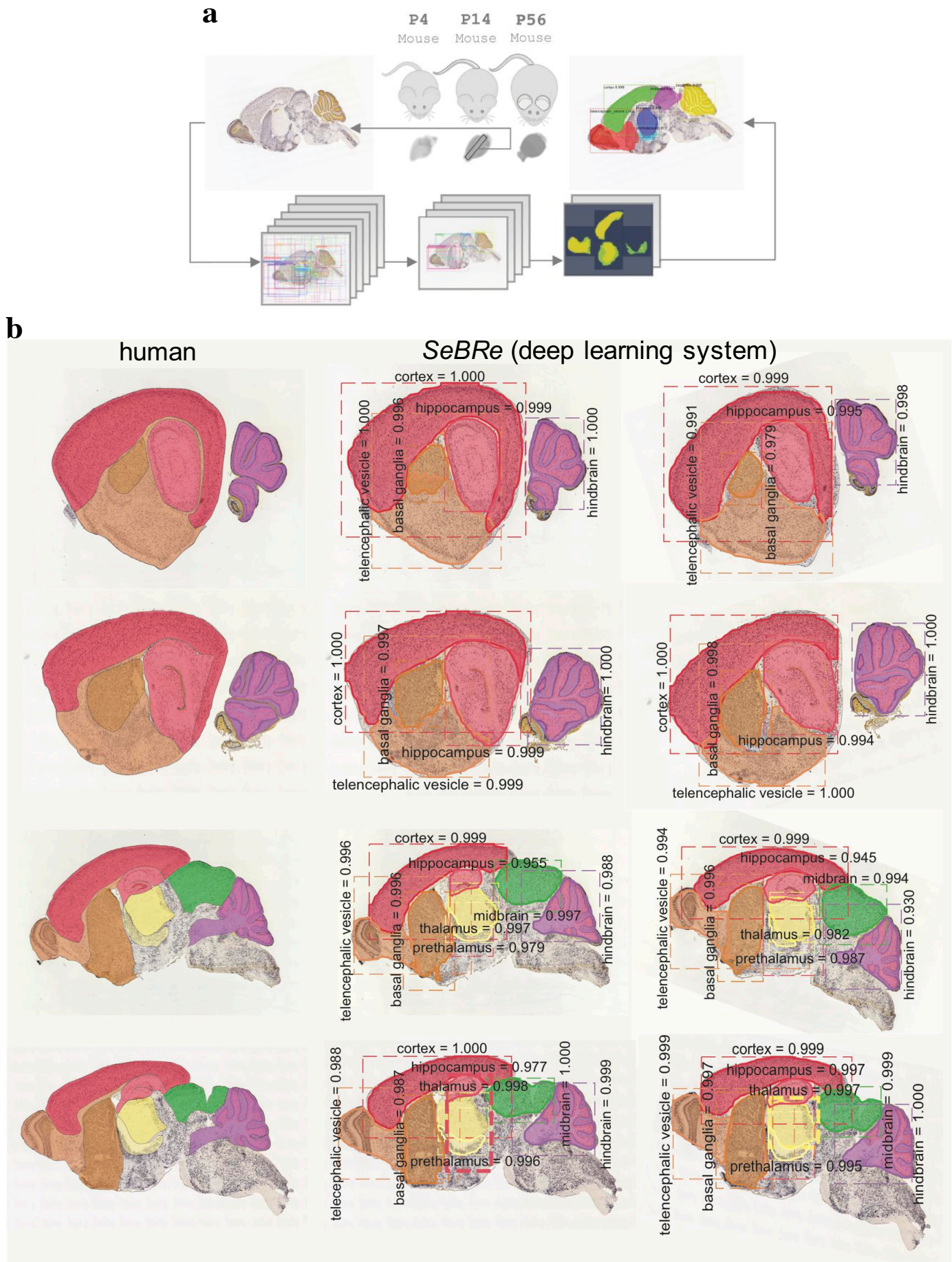


Fig. 1 | Block Diagram and performance of SeBRe. **a**, Block diagram architecture of SeBRe. Brain sections (left) are fed as input to the Mask RCNN and the output (right) shows the segmented (registered) brain regions on top of the input brain section. **b**, Qualitative performance comparison of SeBRe on lateral (rows 1-2) and medial (rows 3-4) brain sections with human-annotated masks. SeBRe performs optimally on predicting masks of brain regions, for both upright (column 2) and rotated (column 3) versions of input brain sections.

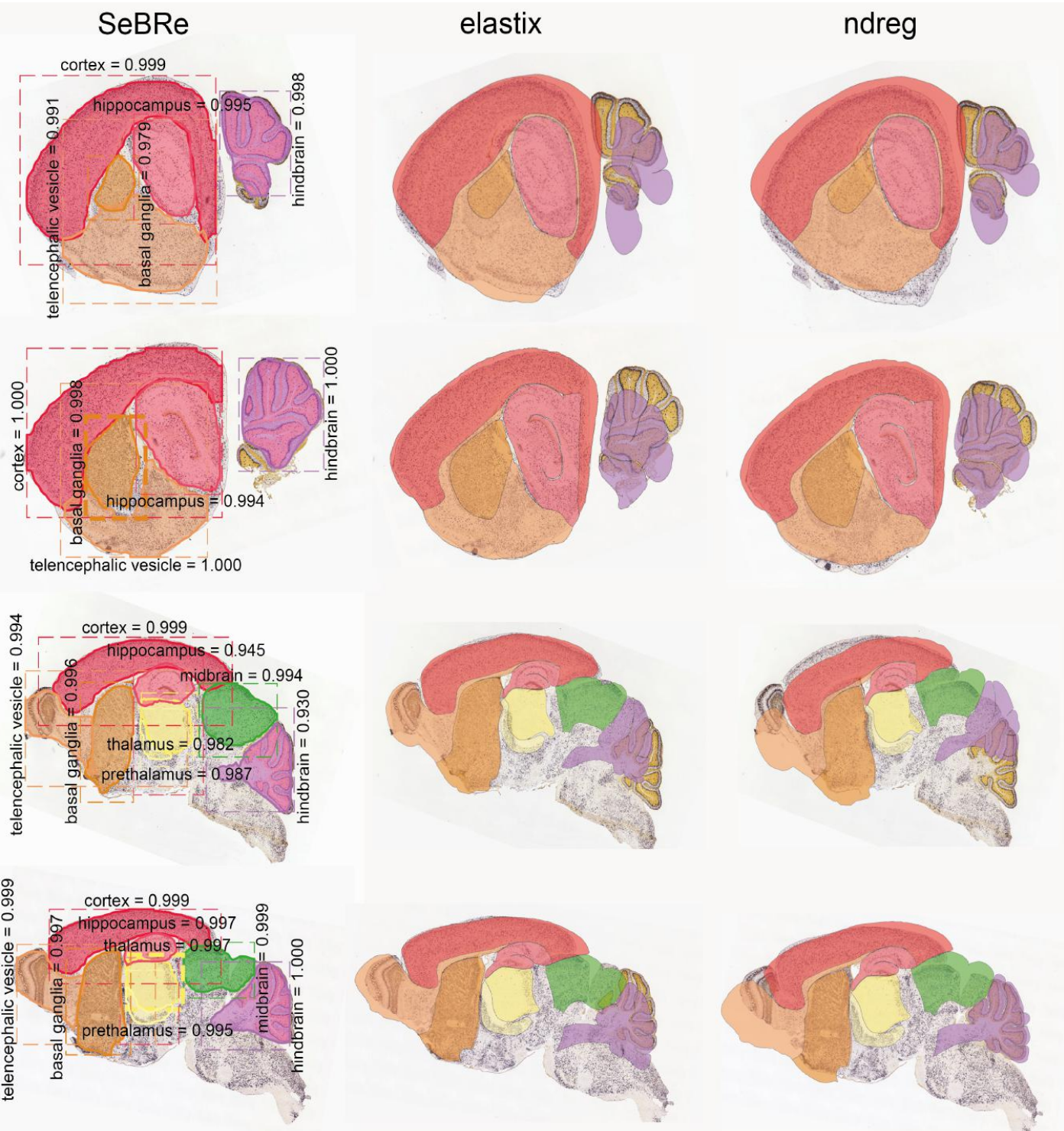
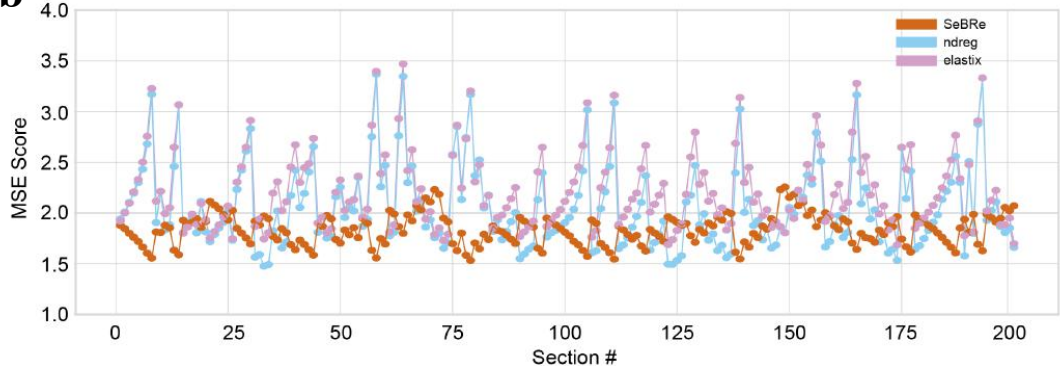
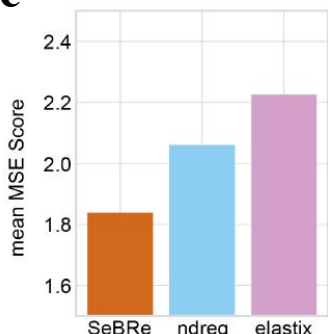
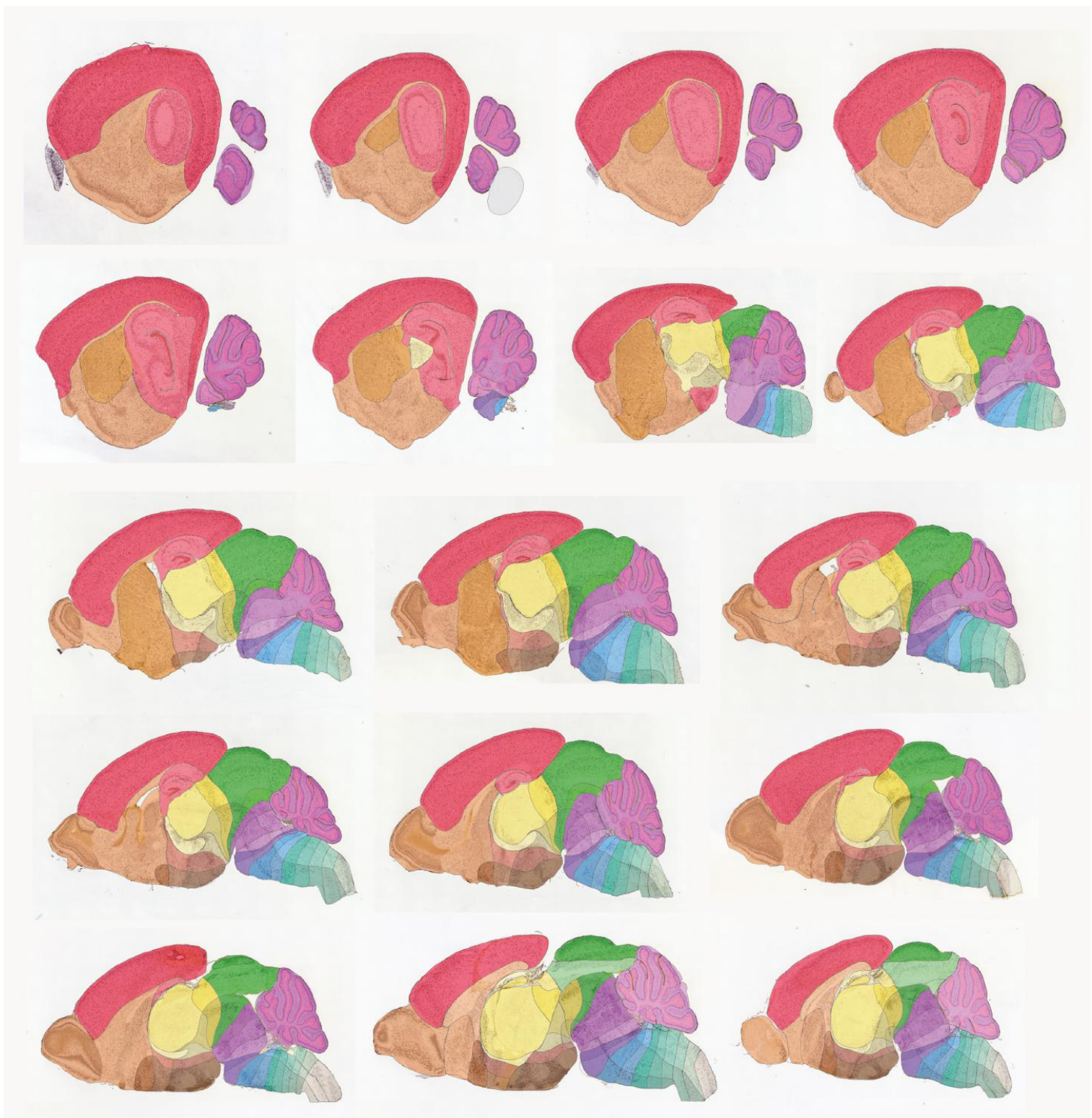
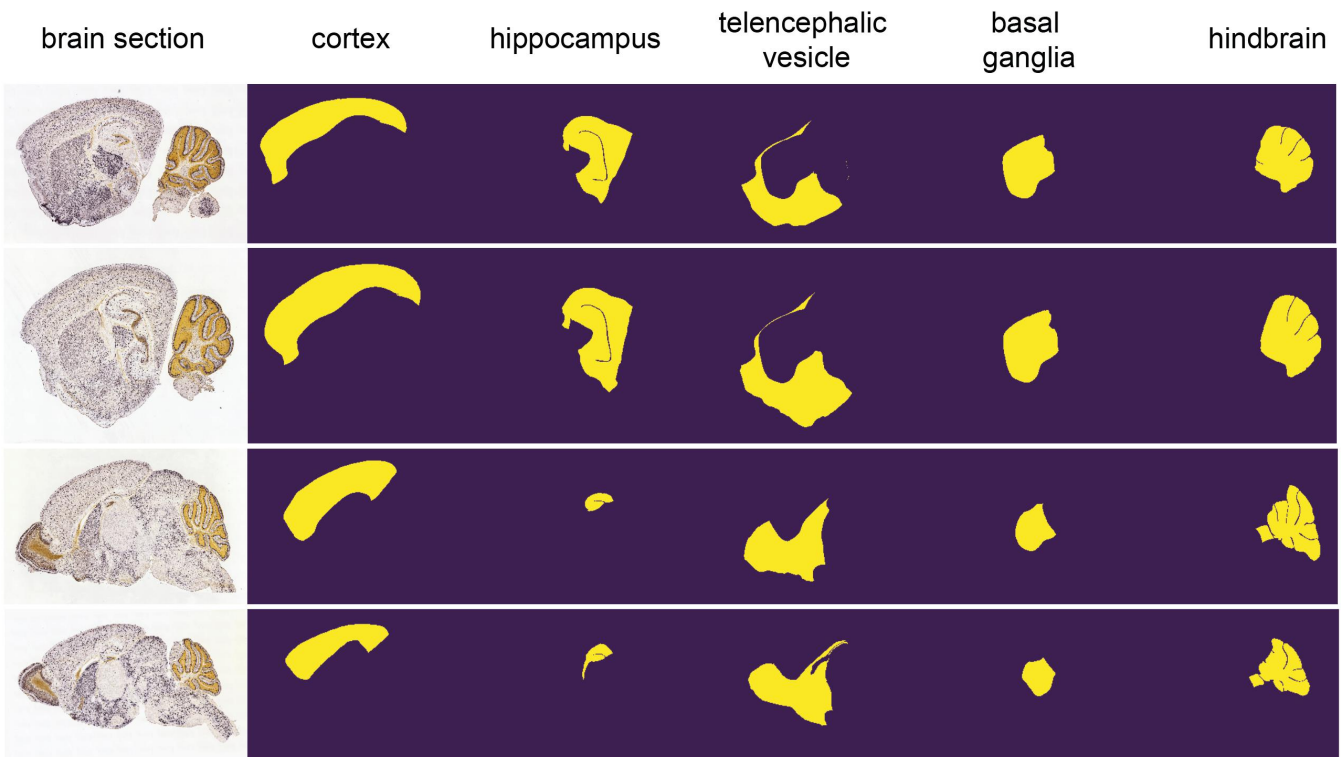
a**b****c**

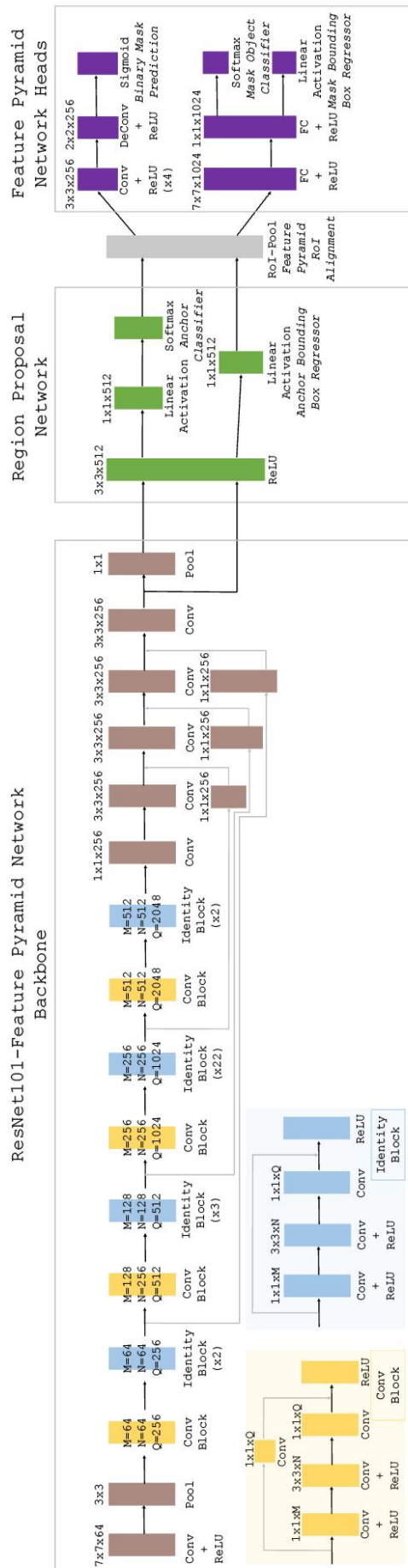
Fig. 2 | Performance comparison of *SeBRe* with commonly used brain registration methods. **a**, Performance of *SeBRe* in predicting brain regions on randomly selected lateral and medial brain sections in comparison with *ndreg* and *elastix* methods. **b**, Plot of MSE scores for all brain sections in the testing dataset, for *SeBRe*, *ndreg*, and *elastix*. **c**, Mean MSE scores for *SeBRe*, *ndreg* and *elastix*, on the complete testing dataset.



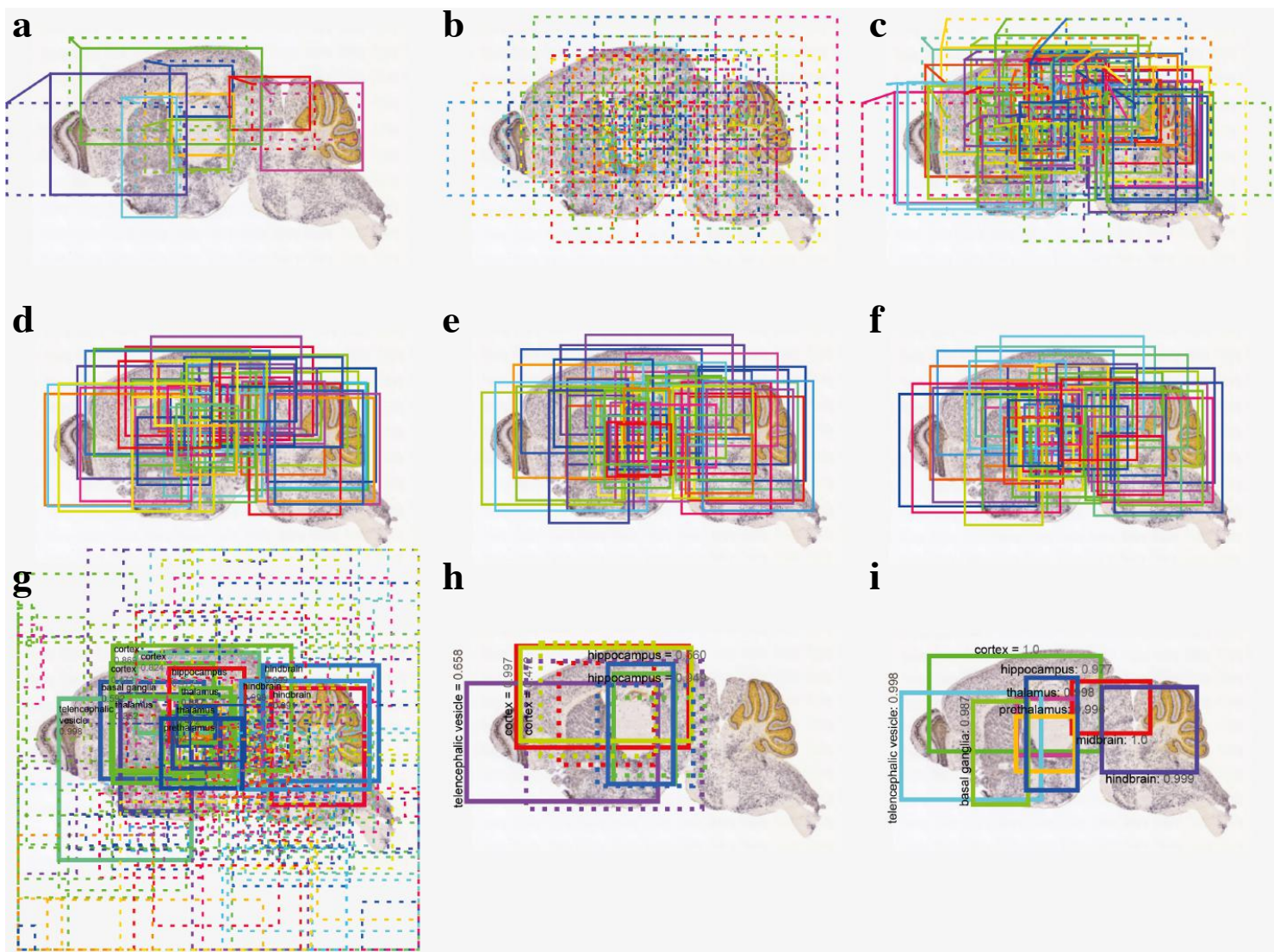
Supplementary Figure 1 | Manually-registered ground-truth data. P14 GAD1 sagittal sections with overlaid Allen developing mouse brain reference atlas. Lateral-most (top left) to medial-most (bottom right).



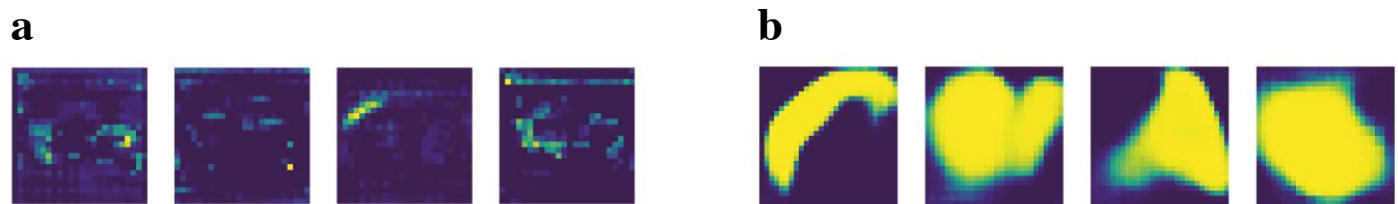
Supplementary Figure 2 | Masks of brain regions on lateral and medial sagittal sections of P14 GAD1 and VGAT ground-truth mouse brains. The first two rows of column 1 show the lateral whereas the last two rows show the medial brain sections. Column 2-6 show the ground-truth masks of five example brain regions. The regions vary in shape and size as we move from lateral to medial (e.g. compare hippocampus across column 3, for all brain sections).



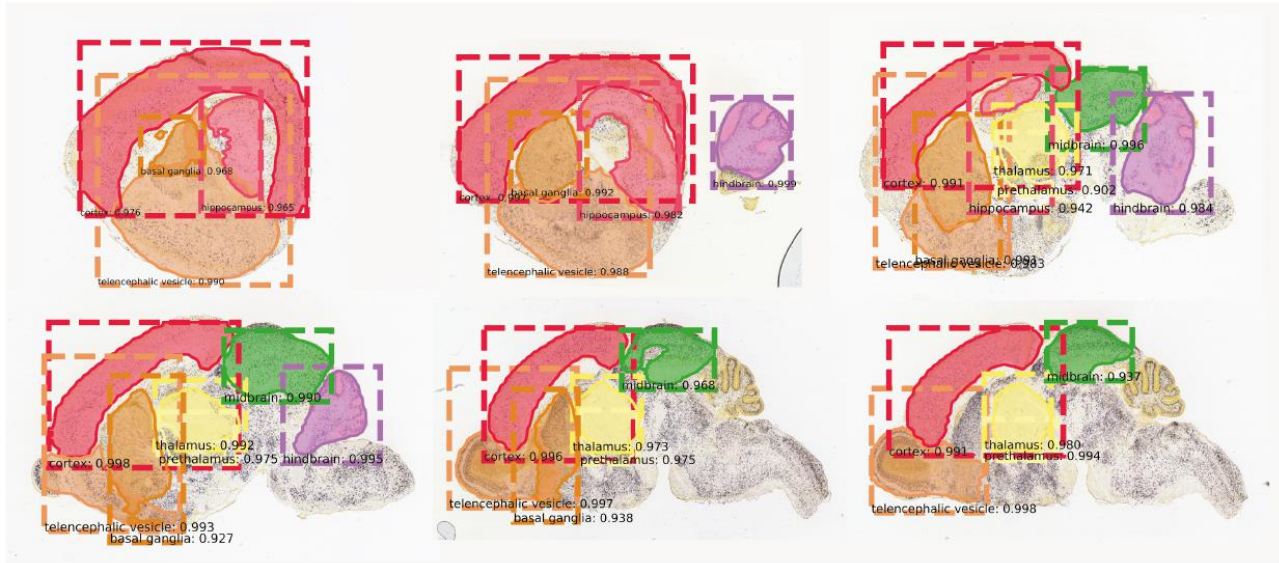
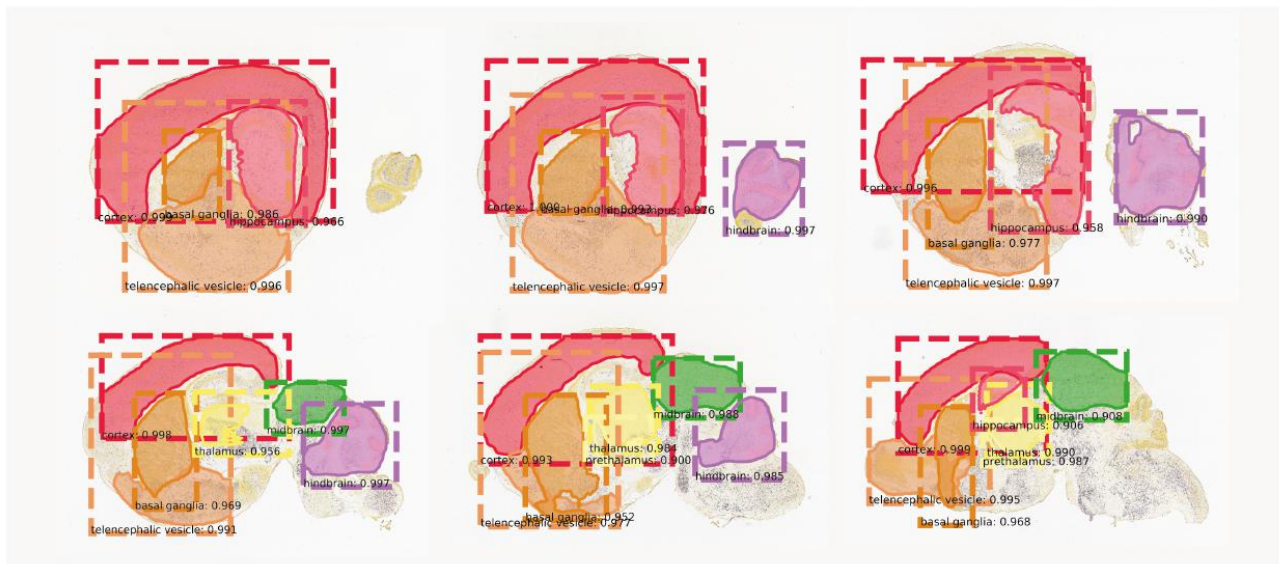
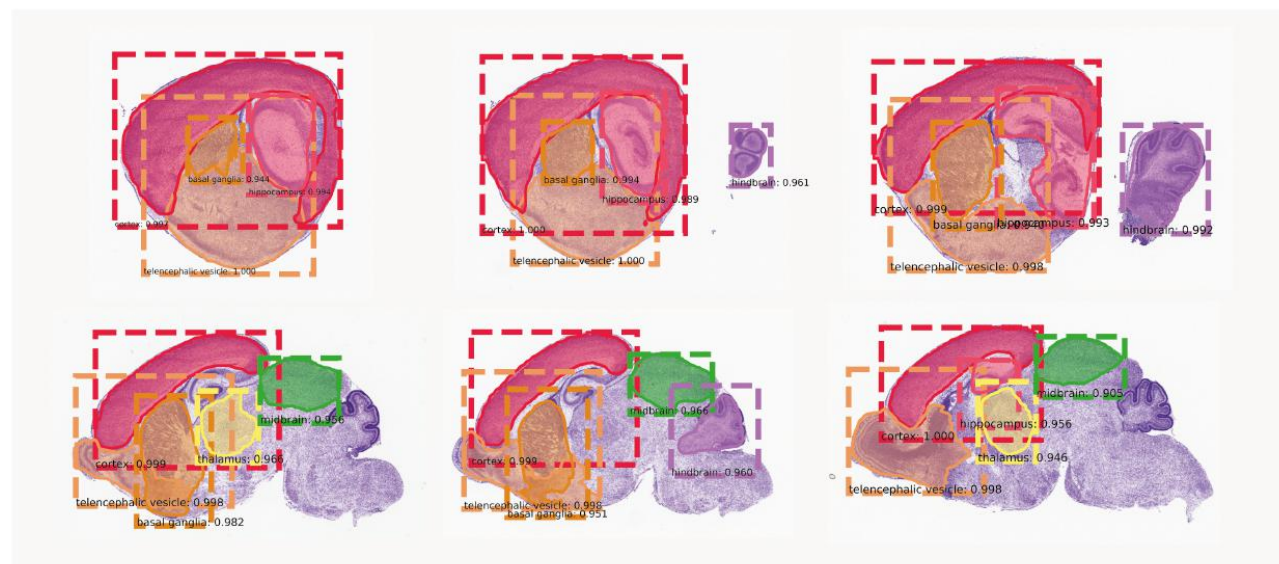
Supplementary Fig. 3 | SeBRe architecture. A multistage Mask RCNN network, based on ResNet-101 and FPN as backbone architecture is developed. The output of ResNet-FPN is fed to the RPN, where brain regions are localized and bounding boxes for RoIs are proposed. The proposed feature maps are down-sampled in the RoI pooling layer (RoIAcc layer), followed by the FPN heads where binary masks are proposed and brain regions are segmented pixel wise.



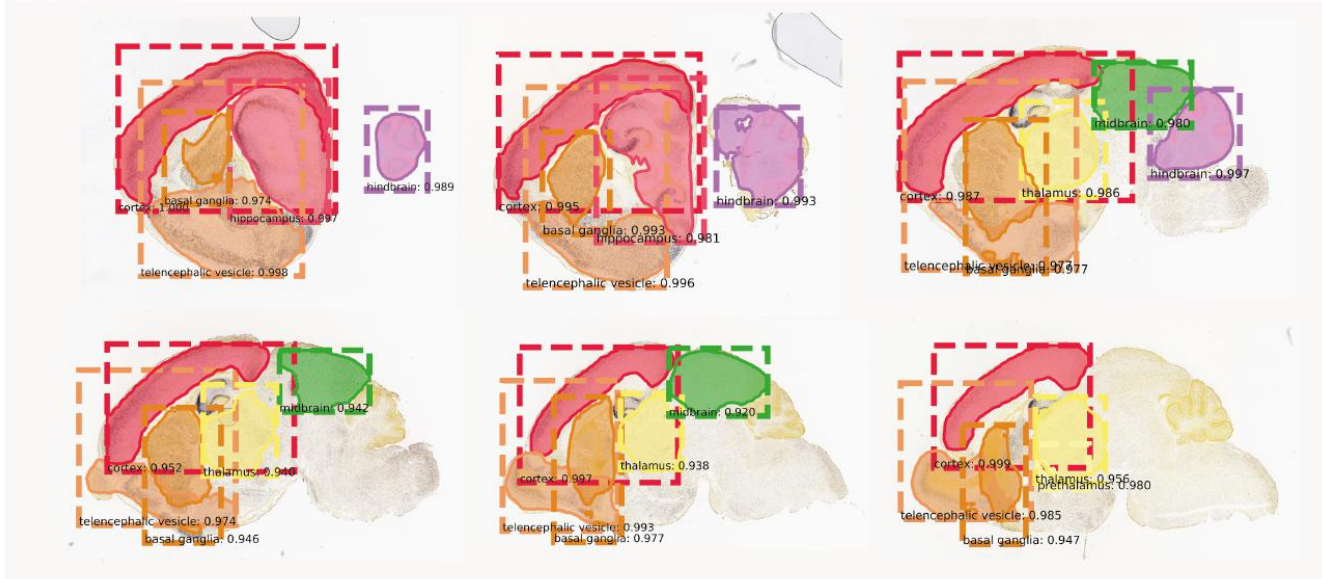
Supplementary Figure 4 | SeBRe multistage image processing pipeline. Step-by-step flow of brain region localization (a-f) and classification (g-i): **a**, the bounding boxes of ground-truth targets, generated for Region Proposal Network (RPN) training. **b**, boxes for proposed regions (anchors) predicted by the RPN. **c**, the RPN-predicted anchors after refinement. **d**, the RPN-predicted anchors after clipping to image boundaries. **e**, the RPN-predicted anchors after applying non-maximum suppression. **f**, final predicted anchors shown after coordinate normalization. **g**, predictions of the Feature Pyramid Network (FPN) classifier heads, on RPN-predicted anchors, before refinement (boxes are labelled with predicted class and confidence score; dotted boxes represent proposals classified as background). **h**, FPN-predicted classes after anchor refinement and non- maximum suppression. **i**, final brain region detections of the FPN regressor and classifier heads.



Supplementary Fig. 5 | Output feature maps at different stages of *SeBRe* image processing pipeline. **a**, Activations of feature maps produced by the ResNet101-FPN backbone architecture. **b**, Output feature maps of the FPN head, predicting the region-wise masks of brain sections.

a P4 GAD1**b P4 VGAT****c P4 Nissl**

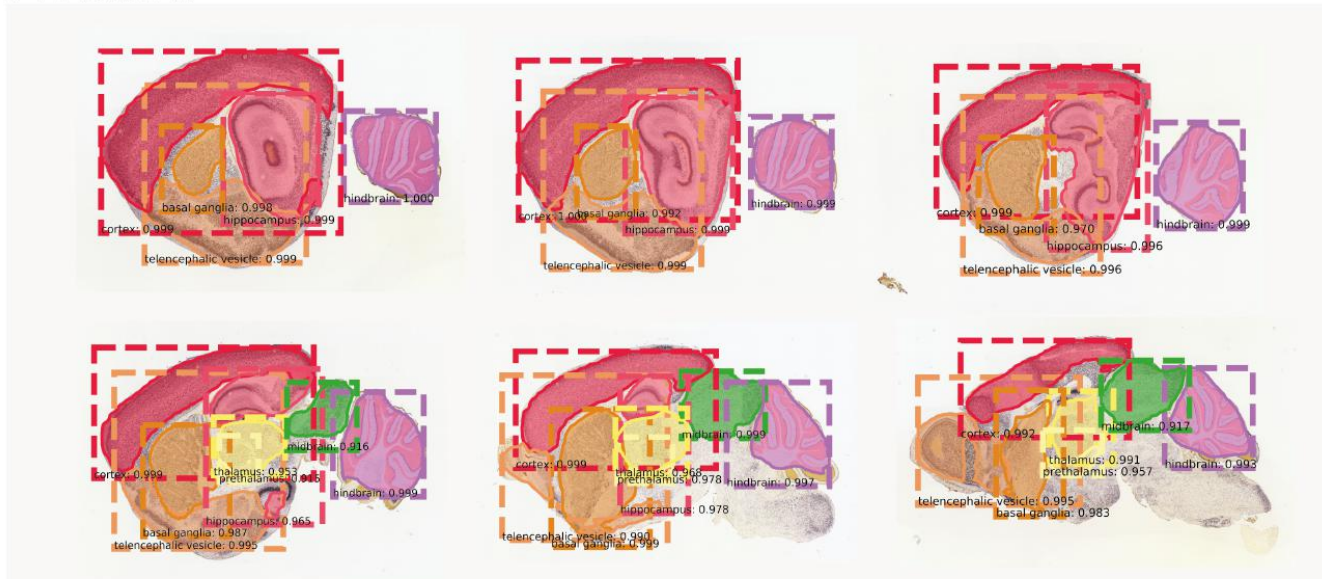
d P4 CamKII



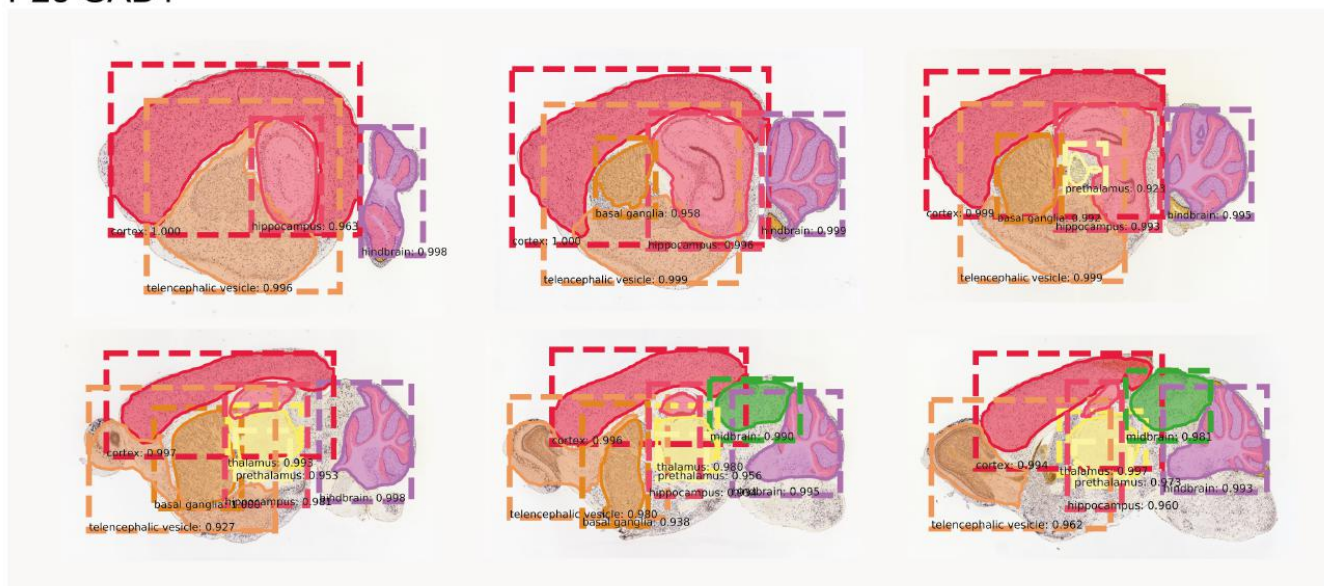
e P14 Nissl



f P14 CamKII



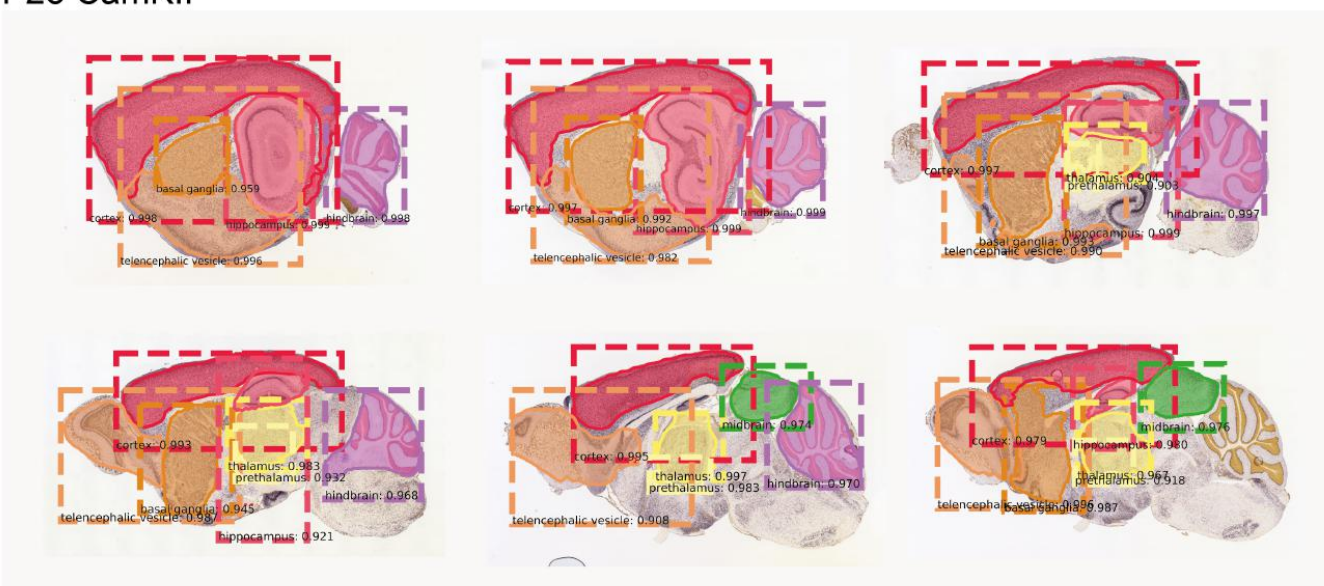
g P28 GAD1



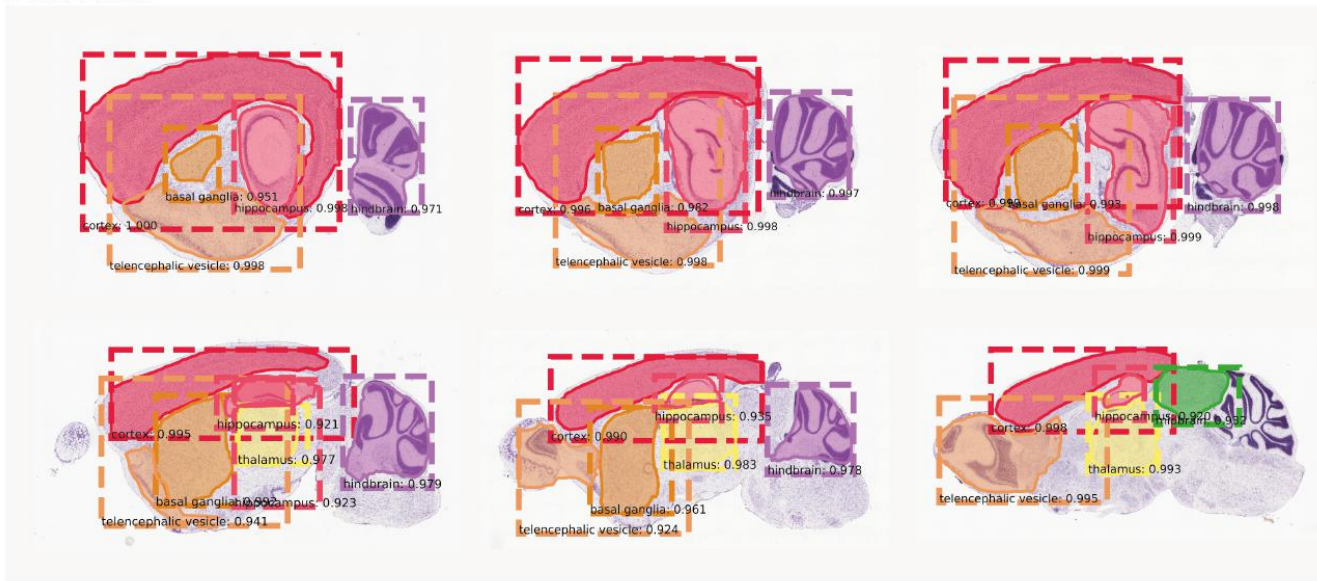
h P28 VGAT



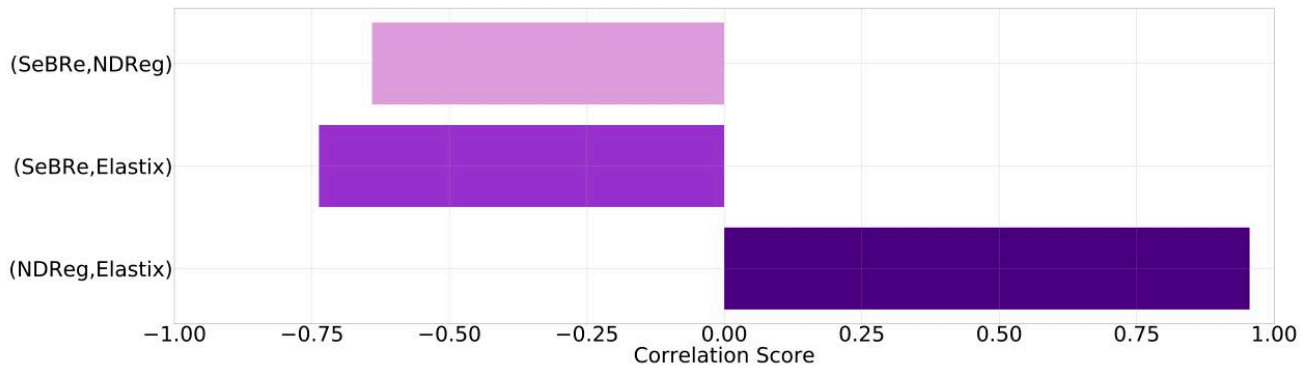
i P28 CamKII



j P56 Nissl



Supplementary Figure 6 | Performance of *SeBRe* on various ‘unseen’ mouse brain ISH tissues, across different developmental time points. a, Predicting masks of brain regions by *SeBRe* on GAD1 brain sections at age P4. b, on VGAT at age P4, c, on Nissl at age P4, d, on CamKII at age P4, e, on Nissl at age P14, f, on CamKII at age P14, g, on GAD1 at age P28, h, on VGAT at age P28, i, on CamKII at age P28 and j, on Nissl at age P56.



Supplementary Figure 7 | Pairwise correlation of *SeBRe*, *ndreg* and *elastix* MSE scores on testing dataset. It appears that *ndreg* and *elastix* have a strong positive correlation in their MSE scores on the complete testing dataset of brain regions. However, interestingly, *SeBRe* is negatively correlated with these methods. The plot points towards the fact that the drop in the performance of *SeBRe*, which mainly occurs due to the brain regions omitted by the network, is very different from the errors made by *ndreg* and *elastix* in registering the brain sections. Since, *ndreg* and *elastix* utilize affine and non-affine transformation algorithms and therefore cannot minimize error by omitting regions, they instead map the reference atlas incorrectly during registration, which undermines performance.